Device Design for the Rapid Ultrasonic Rewarming of Alginate Beads and Cryoprotectant Solution to Improve Cryopreservation Recovery

Rui Xu[1,2], Thomas Brookshaw[3], Eloy Erro[3], Morgan Roberts[1], Clare Selden[3], Eleanor Martin[1,2]
1. *Department of Medical Physics and Biomedical Engineering, University College London*
2. *Wellcome / EPSRC Centre for Interventional and Surgical Sciences, University College London*
3. *Institute for Liver and Digestive Health, Division of Medicine, Royal Free Hospital, University College London*
rui.xu@ucl.ac.uk, elly.martin@ucl.ac.uk

***Abstract*—Ultrasonic rewarming is a new method for improving cryopreservation recovery. We developed an ultrasonic rewarming device and control algorithm for the rapid and repeatable rewarming of cryopreserved biological media in cryovials. We characterised the device's acoustic output with hydrophone measurements and rewarming rates with thermocouple measurements. Mean rewarming rates of 120°C/min were achieved with cryopreserved alginate beads and cryoprotectant solution. The ultrasound exposures implemented free-field pressure amplitudes in the 3 MPa range, corresponding to 100 W electrical absorbed power. The exposure duration timing was accurate to ∼0.5 s. The device will provide a platform for ultrasonic rewarming cell viability studies.**

***Index Terms*—Focused Ultrasound, Rewarming, Device Design**

I. Introduction

New methods are being developed to enhance the recovery of cryopreserved media from low temperature storage by increasing rewarming rates beyond those achieved with current standard methods [1, 2, 3, 4]. Faster rewarming can reduce exposure to the high sub-zero temperatures associated with ice crystal growth and cell damage. Initial studies show that ultrasound can rewarm biological media, with potential advantages over radiofrequency or inductive rewarming methods [1, 2]. Ultrasonic rewarming may be particularly effective for large thermal conduction-limited volumes that recovery poorly with current methods [5]. However, cell studies are needed to understand the effects of the high pressures required for rapid ultrasonic rewarming, and commercial ultrasonic rewarming devices have not yet been developed.

We previously developed a device for ultrasonic rewarming of biological tissue in 2 ml cryovials to demonstrate the concept of ultrasonic rewarming [1]. This device used a nylon 6.6 coupling block between the transducer and the cryovial, which has a similar acoustic impedance to the propylene cryovial. However, to allow for thermal expansion, a water-filled gap between the transducer and coupling block was needed. This affected transmission of ultrasound to the sample, resulting in substantial transducer self-heating and causing changes in its electromechanical properties [6], resulting in high variability in rewarming rates. The device was also manually controlled, which increased variability in rewarming.

This paper describes development and characterisation of a second prototype device for the reproducible and controllable warming of cells contained in cryovials. To achieve this, the design criteria were:

- robust and efficient acoustic coupling,
- repeatable and user-friendly cryovial positioning, and
- automated exposure control.

Once constructed, the system was acoustically characterised, and warming rates of alginate beads and cryoprotectant solution (ABCPS) were measured. A potential application of ultrasonic rewarming is the recovery of the large volumes of alginate encapsulated liver spheroids required for a BioArtificial liver device [7]. The ABCPS mixture is stable and was therefore chosen as a mimic for this cell preparation for device characterisation.

II. Device Design

The rewarming device was designed around a tubular transducer element (66 mm inner diameter, 76 mm outer diameter, 50 mm height) made from a proprietary PIC181 lead zirconate-lead titanate ceramic (PI Ceramic, Lederhose, Germany) [1, 6]. The density ρ of the transducer element is 7850 kg/m^3, and the sound speed c, determined from the elastic stiffness coefficient C_{33}^D (1.664×10^{11} N/m^2), is calculated as $c = \sqrt{C_{33}^D/\rho} = 4604$ m/s [6]. This results in an acoustic impedance of 36.1 MRayl.

A. Acoustic Coupling

Two coupling fluids were tested as replacements for the previously-used nylon 6.6 coupling block:

1) de-ionized water: ubiquitous in ultrasound research
2) aqueous glycerol: well characterised, miscible in all proportions with water up to the acoustic impedance of polypropylene [8, 9]

Without matching, the acoustic impedance mismatch between the PIC181 transducer and coupling fluid reduces intensity transmission to approximately 20% [10]. However, a

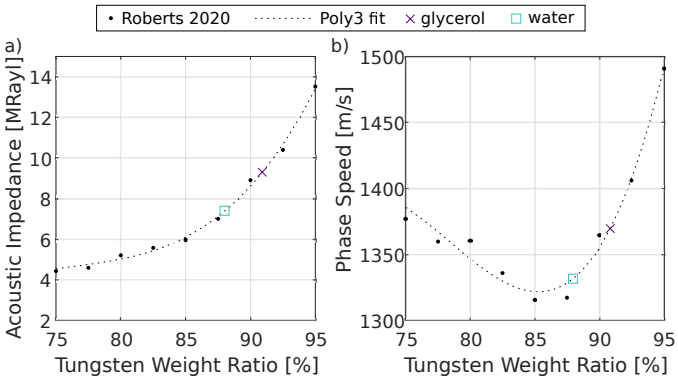

Fig. 1. a) Acoustic impedance measurements [13] were interpolated to identify the tungsten weight ratios to match PIC181 to glycerol or water. b) The thickness of the quarter-wavelength matching layer was calculated from interpolated phase speed measurements, made at 2 MHz.

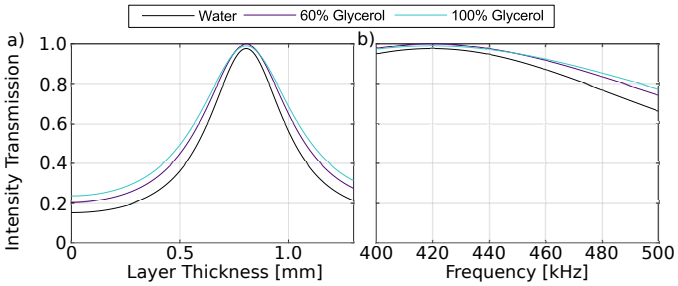

Fig. 2. a) The effect of layer thickness on intensity transmission for a 420 kHz wave from the PIC181 transducer to water, aqueous glycerol and glycerol, and b) intensity transmission between 400 and 500 kHz for a 0.806 mm matching layer.

quarter-wavelength acoustic matching layer can largely negate intensity transmission loss through an interface between materials with acoustic impedances Z_1 and Z_3 [10]. At 25°C and normal ambient pressure, Z_3 is equal to approximately 1.5 MRayl for water [11, 12] and 2.4 MRayl for >99.5% glycerol [8], resulting in Z_2 of 7.4 MRayl and 9.3 MRayl, for water and glycerol, respectively. An epoxy (Araldite®, Huntsman Advanced Materials, Cambridge, UK) - tungsten powder (Tungsten Alloys, London, UK) composite was selected for the acoustic matching layer. The acoustic properties of this composite have been characterised for a range of tungsten weight ratios [13]. The experimental data in [13] were interpolated to identify the tungsten weight ratio which has the desired impedance for matching to water and glycerol. The required thickness of the matching layer at the theoretical resonant frequency of the rewarming transducer, 420 kHz [1, 6] was then calculated from the phase speed of this ratio, as shown in Fig. 1a).

The optimal tungsten weight ratios were 88% for water and 90.9% for glycerol. In practice, it is challenging to obtain a tungsten weight fraction above 90% in the required ∼60 ml volume. An intermediate tungsten weight ratio of 89.9% was therefore chosen, with an acoustic impedance of 8.54 MRayl and phase speed of 1353 m/s, and mixed to give a sufficient volume to coat the internal surface of the tubular transducer with a 3 mm layer. The total mass of the tungsten-epoxy composite was 248.55 g, consisting of 25.10 g epoxy (13.94 g resin and 11.16 g hardener) and 223.45 g tungsten powder. Tungsten powder was mixed into the epoxy in four parts. The composite was then applied manually to the internal transducer surface. The composite viscosity was high so did not require support during the 48 hr curing period. The cured composite layer was then machined to a uniform thickness of 0.806 mm, matched to 60% glycerol at 420 kHz. Fig. 2 displays the calculated relative transducer output against matching layer thickness and frequency. The chosen intermediate impedance is well suited to the both water and pure glycerol, and both have similar optimal layer thicknesses [10]. The matching layer improves relative intensity transmission by at least a factor of three at frequencies up to 480 kHz, allowing variation of driving frequency to optimise tube resonance without substantial reflective losses.

B. Device Housing

A device housing was designed to externally seal the base of the transducer using an o-ring (75 mm diameter, 2 mm cross-section) in a groove (1.85 mm depth, 2.5 mm height) [14] to contain the fluid coupling medium. The device housing was 3D printed using polylactic acid filament then sealed with grease. A cryovial mount was designed and 3D printed for the sliding-fit insertion of the 2 ml Nunc™ CryoTube™ cryovials (Thermo Fisher Scientific, Roskilde, Denmark), radially centering the cryovials within the acoustic field. The sliding-fit design allows for simple and accurate cryovial insertion and easy removal from the rewarming device, while minimizing the disruption of the acoustic field within the transducer volume. The volume external to the transducer and within the housing was filled with low-density polyutherane foam (CRC, Hormsham, PA, USA), effectively air-backing the transducer to maximize continuous-mode sonication efficiency. This also provides electrical insulation and prevents user access to the external transducer electrode. A BNC cable was soldered to the internal and external silver electrodes, and a T-type thermocouple (Omega, 5SRTC-TT-T-36-72, Norwalk, USA) was attached to the external transducer surface with epoxy resin to monitor transducer temperature. The transducer and housing is pictured in Fig. 3.

III. Device Monitoring and Control

The transducer is driven with a signal generator (Keysight 33500B, Santa Rosa, CA), which was connected to a workstation via USB and controlled using VISA interface code from the Matlab instrument control toolbox. The drive signals are amplified by an E&I 1020L 200 W power amplifier (Rochester, NY). An NRT power reflection meter and NAP-Z8 power head (Rhode & Schwarz, Germany) measures the amplifier power output and is connected to the workstation via GPIB and controlled using serial commands. Transducer and cryovial temperatures are monitored with T-type thermocouples (probe diameter: 0.076 mm, Omega 5SRTC-TT-T-36-72), using an

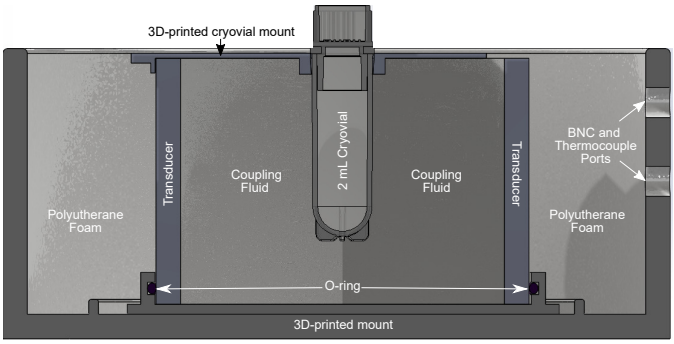

Fig. 3. The transducer is housed within a 3D-printed mount, sealed with an o-ring to contain the acoustic coupling fluid, and air-foam backed.

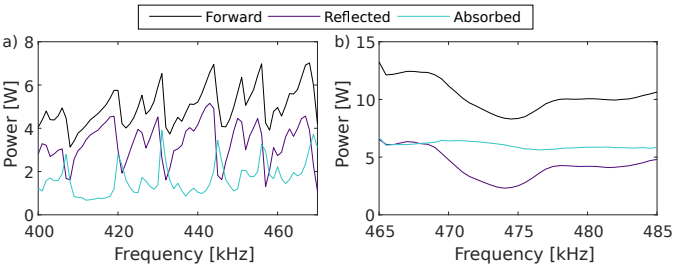

Fig. 4. Forward, reflected, and absorbed power with a) aqueous glycerol and b) deionized water as the coupling fluid. Frequency selection was based on maximising absorbed power and minimising reflected power.

eight-channel Pico Technology TC-08 USB datalogger (Pico Technology, Cambridgeshire, UK), controlled via code from the Matlab File Exchange [15]. The maximum sampling rate of the power reflection meter in continuous wave mode is 2 Hz, which dictates the sampling rate of the thermocouple datalogger and the update rate of the signal generator.

The tubular transducer acts as a resonant cavity with the chosen coupling medium, so careful frequency selection is needed to maximise transducer efficiency with the chosen coupling fluid and fluid temperature. An automated frequency sweep (See Fig. 4) was performed to identify the maximum absorbed electrical power in the range from 400 to 470 kHz in 1 kHz steps, with 60% aqueous glycerol coupling (Fig. 5a), and between 465 and 485 kHz with deionized water (Fig. 5b). 434 kHz and 474 kHz were selected from the measurements for later experiments with aqueous glycerol and deionized water, respectively. The heating rate of pure glycerol contained in a cryovial was measured over the 400 to 450 kHz frequency range using a radially centered thermocouple. 5 s continuous-wave sonications at constant driving amplitude were performed at each frequency with a 30 s cooling period between each. The temperature trace heatmap in Fig. 5a) was averaged across the 5 s exposures at each frequency to obtain the heating rates. Higher heating rates occur at frequencies where absorbed power is also high as shown in Fig. 5b,c). There is a difference of two orders of magnitude in the heating rate at the most and least efficient frequency tested.

Pure (>99.5%) glycerol and polypropylene both have an

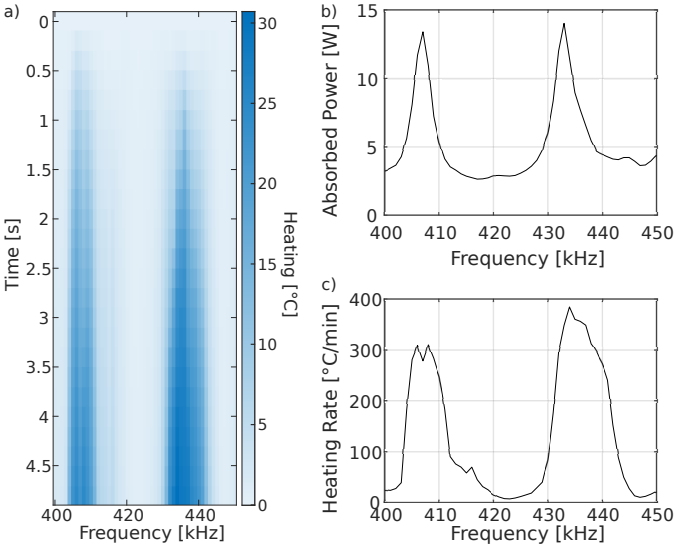

Fig. 5. a) Thermocouple measurements of heating in a glycerol filled cryovial during 5 s sonications (400 to 450 kHz in 1 kHz steps). Maxima in absorbed power during these sonications, (b) correspond to maximum heating rates, (c).

acoustic impedance of 2.4 MRayl [8, 9], making pure glycerol attractive as a coupling medium. However, high attenuation in pure glycerol gives e.g., 60% aqueous glycerol an advantage in a resonant cavity. Aqueous glycerol sound speed depends on glycerol weight fraction [8], so repeated experiments require careful measurement of initial water/glycerol proportions and minimal atmospheric exposure; glycerol is hygroscopic. For example, a 1% difference in glycerol weight fraction (65% to 66%) changes the resonance mode near 440 kHz by 1.2 kHz and would significantly affect device efficiency. De-ionized water is acoustically stable by comparison, easy to use, similarly well acoustically matched, and was thus used for later experiments where replicability across experiments was important.

To ensure repeatable ultrasound exposures during rewarming, a control algorithm was created to automate exposure timing and control the transducer power output in response to changes in transducer thermoacoustic properties due to self-heating.

Exposure timing was automated, starting upon cryovial insertion and lasting for a specified time. Exposure is initiated by detecting the insertion of the cryovial via an electroacoustic effect observed during the characterisation of the voltage to electrical power relationship, with and without a cryovial (containing room-temperature ABCPS) inserted into the device. This characterisation was performed at 474 kHz (optimised for de-ionized water), and with the system heated to 33°C.

The absorbed electrical power for a given voltage is substantially higher when a cryovial is present compared to when there is only water as shown in Fig. 6a); this effect enables detection of the cryovial insertion to automatically trigger the exposure. The full control algorithm is depicted as a flowchart in Fig. 6d). The exposure timing control is as follows. The device is initiated at a low driving voltage, and absorbed

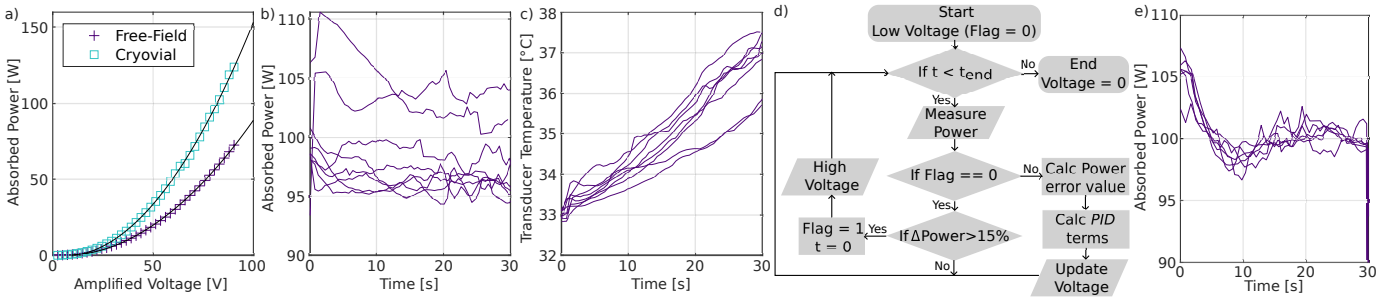

Fig. 6. a) Absorbed electrical power varies quadratically with input voltage, and with cryovial insertion. This relationship is used to select a driving voltage for a desired power, e.g. b) 100 W, but results in time-varying power due to changes in the transducer and cavity acoustic properties. Some of the error in b) may result from differences in system temperature (c). d) Rewarming device flowchart. e) Measured power during a 30 s sonication, with a proportional-integral-derivative (PID) controller correcting towards 100 W.

electrical power is sampled at 2 Hz. A change in power of more than 15% triggers the system to increase the signal generator voltage to start rewarming at the desired power using the relationship shown in Fig. 6a), and starts a timer for the desired exposure duration. The device shuts off once the timer expires. This algorithm results in exposure times consistent to within ∼0.5 seconds.

Without active control, absorbed electrical power will vary during sonication due to transducer self-heating and changes in the properties of thawing samples [1]. Transducer temperature and absorbed power was measured during warming of cryovials containing ABCPS cooled to -80°C in a controlled rate freezer (Asymptote, UK). Warming was repeated eight times for 30 s at a set power of 100 W. Transducer temperature increased by up to 5°C (Fig. 6c) and the average absolute error in absorbed power was 3.5 W with a peak error of 10.6 W (Fig. 6b).

A proportional-integral-derivative (PID) controller was implemented to control driving voltage to minimise the difference between the measured absorbed electrical power and the desired power. The PID terms were chosen empirically based on a set of rewarming experiments. Values of proportional gain, $K_p = 0.002$, integral gain, $K_i = 0.001$, and derivative (damping) gain, $K_d = 0.001$ were found to produce stable corrections.

The PID controller was implemented as shown in the flowchart in Fig. 6d). Once high power sonication is initiated, absorbed power is measured at 2 Hz, and the difference between measured power and set power is used to obtain a voltage correction. After implementation of the PID controller, rewarming sonications were repeated as previously (Figure 6e). The average absolute error in absorbed power was reduced to 1.2 W, one third of the error without control, demonstrating a substantial improvement in reproducibility between trials.

IV. Device Characterisation

A. Acoustic Pressure Measurements

The acoustic pressure distribution within the transducer cavity when filled with de-ionized water was characterised using a fibre-optic hydrophone (Precision Acoustics, Dorchester, UK) calibrated against a 0.2 mm capsule hydrophone (Onda, Sunnyvale, CA, USA) and positioned with a 3-axis UMS positioning system (Precision Acoustics Ltd, Dorchester, UK). Pressure was measured in the centre of the cavity where the cryovial would be placed. A lateral line scan was performed at a height of z = 10 mm from the top of the transducer, from -5 to 5 mm about the centre in 0.2 mm steps. An axial scan was performed at the centre from z = 10 to 35 mm in 0.5 mm steps. The driving signal was a 100 cycle pulse with an amplitude corresponding to a continuous-wave electrical power of 52 W. Pressure amplitude was extracted from the final 10 cycles of the pulse, capturing the resonant behaviour of the transducer cavity. The pressure profiles are displayed in Fig. 7a,b). Pressure along the vertical axis is relatively constant, while the lateral pressure profile shows a central peak coincident with position of the centre of the cryovial during rewarming. This pressure profile suggests that rewarming will be fastest at the centre and with a greater contribution from thermal conduction from the coupling fluid at the edges. The width of the central peak depends on the sound speed within the cryovial and will be wider at the higher sound speeds of frozen biological media [1] compared to water.

To characterise the relationship between drive voltage or set power and pressure, the axial scan was repeated at seven voltages which correspond to powers of 0.3 to 110 W. The mean and maximum pressure amplitudes from these scans are displayed in Fig. 7c), reaching mean and maximum vertical axis pressure amplitudes of 3 MPa and 4 MPa respectively, at 100 W. This maximum pressure amplitude is 2.4 times higher than the estimated maximum pressure amplitude achieved with the first version of the device [1]. The acoustic properties of ABCPS remain to be characterised, so the *in situ* pressure cannot be accurately estimated. However, the pressure measurements in water give an upper bound to the expected pressures during rewarming.

B. Rewarming Measurements

Ultrasonic rewarming experiments were completed to investigate the uniformity of rewarming rate throughout the cryovial and to characterise the rate and reproducibility of warming at high driving powers.

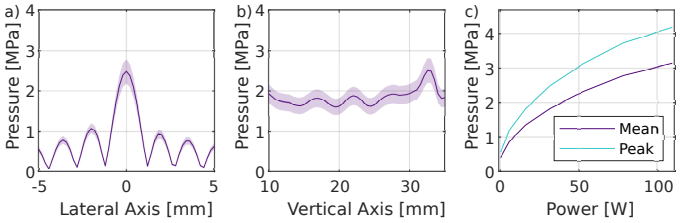

Fig. 7. Pressure profiles measured within the a) lateral span of the cryovial, and b) vertical/axial span of the cryovial volume containing alginate beads + cryoprotectant solution. c) power vs. mean and peak pressure along the axial scans.

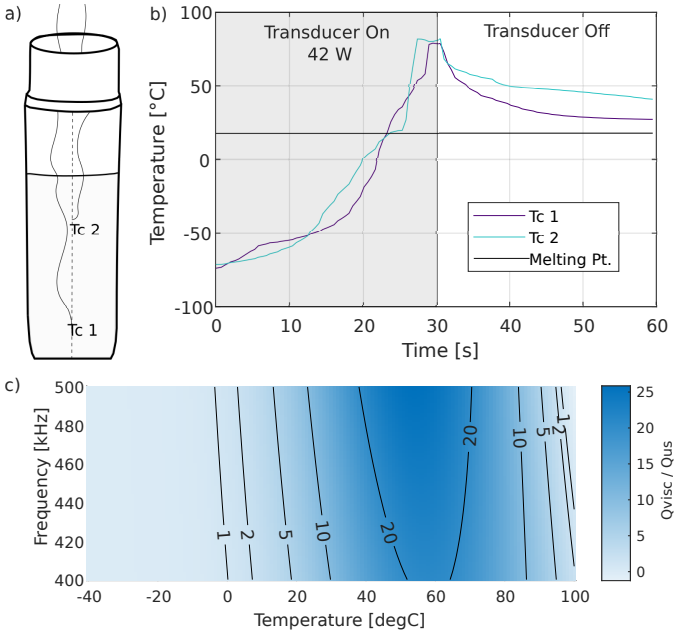

Fig. 8. a) Two thermocouples were strung along the midline of a cryovial containing 100% glycerol. b) Temperature recordings for a 30 s sonication and 30 s cooling, at 42 W absorbed electrical power. c) Estimated ratio of heating from the thermocouple viscous heating artifact (Q_{visc}) [16, 17] in glycerol [18] versus heating from ultrasound absorption (Q_{us}).

Rewarming rates were first characterised with >99.5% glycerol-filled cryovials. Glycerol has been well characterised acoustically and thermally and serves as an inexpensive thermal phantom for cells. A glycerol filled cryovial was cooled to -80°C using a controlled rate freezer, and rewarmed at 434 kHz. Thermocouples were positioned at $r = 0$ and $z = 20$ and 30 mm.

Figure 8 shows that axial rewarming rates are comparable between the two thermocouples, as expected from the measured acoustic pressure profiles shown in Fig. 7b). The rewarming rates were extremely high, particularly for thermocouple 2, between the glycerol melting temperature (17.8°C) and 80°C. This may be attributed to the viscous heating artifact which presents a challenge in thermocouple measurements of acoustic fields [16]. The thermocouple viscous heating artifact magnitude was calculated for glycerol between -40°C and 100°C [16, 8, 18] and compared to the volume rate of heat deposition resulting from ultrasonic attenuation. Fig. 8c) shows

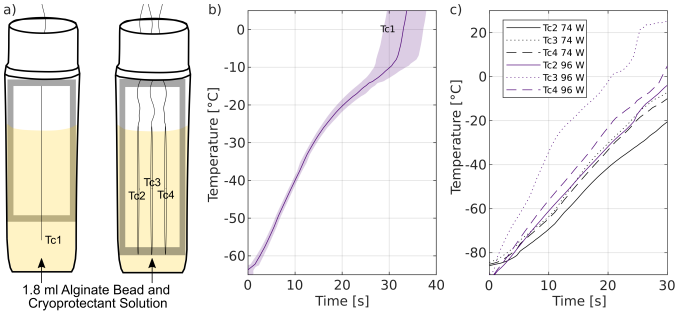

Fig. 9. a) Thermocouple measurements were made in cryovials containing 1.8 ml alginate beads and cryoprotectant solution and one thermocouple ($N = 4$) or three lateral thermocouples spaced 2mm apart ($N = 1$). b) Mean $\pm$ standard deviation in heating for cryovials containing one thermocouple, rewarmed at 100W. c) Rewarming curves for 74 W and 94 W ultrasonic rewarming with three thermocouples.

that the estimated contribution of the viscous heating artifact to glycerol heating is between 5 and 25 times higher that of ultrasonic absorption between the glycerol melting point and 80°. Fig. 8c) shows that thermocouple viscous heating is small at low temperatures (highly viscous glycerol, trapped thermocouple) and at high temperatures (low viscosity, limited resistance to thermocouple vibration), and large at intermediate temperatures where the thermocouple can oscillate and viscous friction dissipates energy in the immediate surroundings. The temperature range of interest for ultrasonic rewarming is primarily below the melting point where the artifact is limited. However, the effect is significant for temperature near and above the melting point, so caution is needed when interpreting thermocouple temperature measurements of ultrasonic rewarming in this temperature region.

Next, a set of rewarming experiments were performed with cryovials containing ABCPS with a) one thermocouple positioned on the cryovial central axis or b) three thermocouples, one on axis and two positioned 2 mm either side of the axis. The single thermocouple cryovials were rewarmed at 100 W until the thermocouple temperature reached 5°C ($N = 4$), as shown in Fig. 9b). The triple thermocouple cryovial was rewarmed once at 74 W and once at 94 W, and both for 30 s as shown in Fig. 9c). The ABCPS rewarmed slower than >99.5% glycerol demonstrating that ABCPS is less absorbing. The ABCPS rewarming is constant to the phase change between -15 and -10°C, then the rewarming rate accelerates once the temperature reaches -10°C. The acceleration above the phase transition may be due to a change in acoustic and thermal properties resulting in greater ultrasonic absorption and/or a smaller specific heat capacity, or a change in viscosity that amplifies the thermocouple viscous heating artifact. Acoustic and viscous characterisation of the ABCPS is needed in order to better understand ultrasonic rewarming in this high sub-zero temperature regime.

The mean ABCPS rewarming rate at 100 W was 120°C/min, six times faster than mean rewarming rate of 20°C/min achieved with the first version of the device [1]. The standard deviation in rewarming time to the start of the phase transition

at -15°C is small, ± 1.8 s, then increases beyond the phase transition to ± 4.2 s at 5°C. The increase in uncertainty may result from heterogeneous melting within the cryovial. Figure 9c) shows that the lateral rewarming rate is comparable across positions at 74 W, but the central thermocouple records substantially faster rewarming at 94 W. This demonstrates the interplay between rewarming via thermal conduction from the fluid coupling medium and ultrasonic rewarming. Future studies may optimise the acoustic pressure distribution and magnitude to generate a homogeneous rewarming rate throughout a volume.

V. Summary

We developed a simple ultrasonic rewarming device that reproducibly warms 2 ml volumes of cryopreserved cells at rates of >100°C/min, with automated exposure control. This device provides a platform for the study and further development of ultrasonic rewarming of cryopreserved biological media. In future work, the system will be used to assess post-ultrasonic rewarming viability of cryopreserved encapsulated liver spheroids.

VI. Acknowledgements

This work was supported by a UKRI Future Leaders Fellowship (Grant No. MR/T019166/1), and by the Wellcome/EPSRC Centre for Interventional and Surgical Sciences (WEISS) (203145Z/16/Z). The author has applied for a CC BY public copyright licence to any manuscript version arising from this submission. The authors wish to thank Professor Barry Fuller for helpful discussions on this work, and Simon Hemsley for machining the acoustic matching layer.

References

[1] R. Xu, B. E. Treeby, and E. Martin, "Experiments and simulations demonstrating the rapid ultrasonic rewarming of frozen tissue cryovials," *The Journal of the Acoustical Society of America*, vol. 153, no. 1, pp. 517–528, 2023.

[2] E. Alcalá, L. Encabo, F. Barroso, A. Puentes, I. Risco, and R. Risco, "Sound waves for solving the problem of recrystallization in cryopreservation," *Scientific Reports*, vol. 13, no. 1, p. 7603, 2023.

[3] N. Manuchehrabadi, Z. Gao, J. Zhang, H. L. Ring, Q. Shao, F. Liu, M. McDermott, A. Fok, Y. Rabin, K. G. Brockbank *et al.*, "Improved tissue cryopreservation using inductive heating of magnetic nanoparticles," *Science translational medicine*, vol. 9, no. 379, 2017.

[4] B. Wowk, J. Phan, R. Pagotan, E. Galvez, and G. M. Fahy, "27 mhz constant field dielectric warming of kidneys cryopreserved by vitrification," *Cryobiology*, vol. 115, p. 104893, 2024.

[5] P. Kilbride, S. Lamb, S. Gibbons, J. Bundy, E. Erro, C. Selden, B. Fuller, and J. Morris, "Cryopreservation and re-culture of a 2.3 litre biomass for use in a bioartificial liver device," *PloS one*, vol. 12, no. 8, 2017.

[6] P. ceramic, "Piezoelectric ceramic products: Fundamentals, characteristics and applications," 2021.

[7] C. Selden, J. Bundy, E. Erro, E. Puschmann, M. Miller, D. Kahn, H. Hodgson, B. Fuller, J. Gonzalez-Molina, A. Le Lay *et al.*, "A clinical-scale bioartificial liver, developed for gmp, improved clinical parameters of liver function in porcine liver failure," *Scientific reports*, vol. 7, no. 1, p. 14518, 2017.

[8] W. Slie, A. Donfor Jr, and T. Litovitz, "Ultrasonic shear and longitudinal measurements in aqueous glycerol," *The Journal of Chemical Physics*, vol. 44, no. 10, pp. 3712–3718, 1966.

[9] A. R. Selfridge, "Approximate material properties in isotropic materials," *IEEE transactions on sonics and ultrasonics*, vol. 32, no. 3, pp. 381–394, 1985.

[10] R. S. Cobbold, *Foundations of biomedical ultrasound*. Oxford university press, 2006.

[11] F. E. Jones and G. L. Harris, "Its-90 density of water formulation for volumetric standards calibration," *Journal of research of the National Institute of Standards and Technology*, vol. 97, no. 3, p. 335, 1992.

[12] W. Marczak, "Water as a standard in the measurements of speed of sound in liquids," *the Journal of the Acoustical Society of America*, vol. 102, no. 5, pp. 2776–2779, 1997.

[13] M. Roberts, "Progress towards an open-source, low-cost ultrasound computed tomography research system." KIT Scientific Publishing, 2020.

[14] S. L. Apple, "Apple rubber seal design guide," 1989.

[15] G. Akien, "Pico technology tc-08 usb data acquisition (https://www.mathworks.com/matlabcentral/fileexchange/41800-pico-technology-tc-08-usb-data-acquisition), matlab central file exchange," 2024.

[16] W. J. Fry and R. B. Fry, "Determination of absolute sound levels and acoustic absorption coefficients by thermocouple probes—theory," *The Journal of the Acoustical Society of America*, vol. 26, no. 3, pp. 294–310, 1954.

[17] G. G. Stokes *et al.*, "On the effect of the internal friction of fluids on the motion of pendulums," 1851.

[18] N.-S. Cheng, "Formula for the viscosity of a glycerol-water mixture," *Industrial & engineering chemistry research*, vol. 47, no. 9, pp. 3285–3288, 2008.